SOCAR Proceedings

Fundamental Research

journal home page: http://proceedings.socar.az

COPPER(II) COMPLEXES WITH PYRAZINE-MODULATED TETRAPYRIDYLTRIAMINE LIGANDS: SYNTHESIS, CRYSTAL STRUCTURES, AND ANTIMICROBIAL PROPERTIES

S. Z. Ismayilova[1], R. H. Ismayilov*[1], S. Z. Hamidov[2], M. T. Huseynova[1], L. Sh. Guliyeva[1], V. J. Abdullayev[3], F. F. Valiyev[3], Onur Şahin[4], Chi-How Peng[5]

[1]*Institute of Chemistry, The Ministry of Science and Education of the Republic of Azerbaijan, Baku, Azerbaijan*

[2]*Azerbaijan Technological University, Ganja, Azerbaijan*

[3]*«OilGasScientificResearchProject» Institute, SOCAR, Baku, Azerbaijan*

[4]*Department of Occupational Health & Safety, Sinop University, Türkiye*

[5]*Department of Chemistry, National Taiwan University, Taipei, Taiwan, ROC*

ABSTRACT

Two new mononuclear Cu(II) complexes, $[Cu(H_3pzpz)(NO_3)]\cdot NO_3\cdot H_2O$ (**1**) and $[Cu(H_3tpz)Cl]_2\cdot 2(Cl)\cdot 5H_2O$ (**2**), with pyrazine-modulated oligo- α-pyridylamine ligands N^2-(pyrazin-2-yl)-N^6-(6-(pyrazin-2-ylaminopyridin-2-yl)pyridin-2,6-diamine (H_3pzpz) and N^2-(pyrazin-2-yl)-N^6-(6-(pyridin-2-ylaminopyridin-2-yl)pyridin-2,6-diamine (H_3tpz), have been synthesized, structurally characterized, and their antimicrobial efficacy has been studied. Single-crystal X-ray diffraction revealed that the central Cu(II) atom in complexes **1** and **2** was located in a distorted trigonal bipyramidal geometry. In both complexes, H_3pzpz or H_3tpz acts as a tetradentate ligand; it coordinates the copper(II) ion in an all-anti conformation, and the Cu(II) atom is five-coordinated in a distorted trigonal bipyramidal geometry. The distorted trigonal bipyramidal structures of the compounds are consistent with both the «inverted type» EPR spectra, in which $g_{\parallel}$ is smaller than $g_{\perp}$, and two spin-allowed transitions in the visible region of their electronic spectra. The complexes are built into a three-dimensional network by extensive hydrogen bonding and intermolecular π-π interactions, which stabilize the crystal packing. The antimicrobial efficacy of **1** and **2** was evaluated against *P. aeruginosa, M. phlei, A. niger*, and *P. chrysogenum*. Both complexes demonstrated significant potency, with complex 2 showing superior activity, particularly against P. aeruginosa with an inhibition zone of 26 mm compared to 20 mm for complex **1** (at 100 μg/mL). The sulfur-binding affinity and redox activity of these metal complexes also present potential for neutralizing hydrogen sulfide (H_2S) in petroleum reservoirs and preventing the oxidative degradation of crude oil. Specifically, the catalytic properties of Cu(II) complexes may be utilized as inhibitors or catalysts in hydrocarbon oxidation reactions during petroleum refining processes.

Keywords: modulated oligo-α-aminopyridine ligand; copper complex; hydrogen bonds; supramolecular networks; antimicrobial activity.

Date submitted: 12.03.2026 **Date accepted:** 15.05.2026

1. Introduction

Oligo-α-pyridylamines (Scheme 1), as heterocyclic ligands, are very interesting in the variety of coordination modes of multidentate ligands. The oligo-α-pyridylamine ligands are deprotonated and coordinated to metal in all-syn form in linear extended metal atom chains (EMACs), whereas the all-anti conformation was found in mononuclear complexes [1–6]. The dimer of the free ligand contains the oligo-α-pyridylamines in their anti-syn structure [7]. In order to get longer metal strings, we have recently developed a range of tuned oligo-α-pyridylamido ligands modified with pyrazine, pyrimidine, picoline, and naphthyridine [8–13].

In medical chemistry, pyridine and pyrazine are significant heterocyclic compounds that are frequently employed in the production of pharmaceuticals and other active chemicals [14, 15]. With two nitrogen atoms in its six-membered aromatic ring, pyrazine and its derivatives have emerged as a novel and intriguing foundation for the investigation and advancement of chemical compounds' antibacterial activity [16]. According to the study, pyrazine derivatives have strong antibacterial activity and may effectively act against a variety of bacterial and fungal strains [17]. On the other hand, copper is a necessary trace element in biological processes. Copper complexes exhibiting strong biological activities, including antibacterial, antifungal, and antitumor effects, are gaining attention in medicinal chemistry [18]. Excellent antibacterial and antifungal action is demonstrated

**E-mail:* ismayilov.rayyat@gmail.com

http://dx.doi.org/10.5510/OGP20260201209

by a freshly synthesized copper(II) triazine complex [19]. Furthermore, oligo-α-pyridyl/pyrazylamine ligands, particularly their complexes with transition metals that incorporate highly biologically active pyridine and pyrazine rings, are anticipated to demonstrate a range of pharmacological effects, including anticancer, antioxidant, and antibacterial activities. In fact, our recent research has demonstrated the remarkable biological activity of coordination polymers of copper(II), mononuclear complexes, and string complexes of nickel(II) with pyrazine-modulated oligo-α-pyridylamino ligands [20-22].

The escalating prevalence of antimicrobial resistance necessitates the development of novel therapeutic agents with unique mechanisms of action [23]. Metal-based antimicrobial compounds, particularly copper(II) complexes, have demonstrated significant potential due to their multi-targeted modes of action, including membrane disruption, protein denaturation, and generation of reactive oxygen species [24]. Nutrient agar (meat extract peptone agar) is a conventional microbiological medium widely employed in antimicrobial susceptibility testing due to its ability to support the growth of diverse microorganisms [25]. This medium provides essential nutrients, including peptones, meat extract, and sodium chloride, creating optimal conditions for microbial proliferation and accurate assessment of antimicrobial activity. Heterocyclic ligands containing pyrazine moieties exhibit diverse biological activities. The coordination of these ligands to copper(II) centers often results in enhanced antimicrobial potency through increased lipophilicity and improved cellular penetration. In the petroleum industry, microbiologically influenced corrosion (MIC) and biological deterioration of crude oil pose serious challenges; therefore, copper-based antimicrobial compounds offer an alternative solution for pipeline disinfection and produced water treatment. Furthermore, pyrazine-based ligands can be employed in the preparation of stable metal-complex catalysts for high-temperature oxidation processes in petroleum upgrading [26].

2. Experimental part

2.1. Materials and measurements

All purchased chemicals and solvents were of analytical grade (Aldrich and Sigma) and used as received. Elemental analyses of carbon, hydrogen, and nitrogen were carried out using a CHNSO FlashEA™ 1112 Automatic Elemental Analyzer. The electronic spectra were recorded as Nujol mulls and in methanol solution on a Specord 50 plus spectrophotometer. IR spectra were measured by the ATR technique (4000–400 cm^{-1}) on an Agilent Cary 630 FTIR spectrophotometer at room temperature. The magnetic measurement was performed on a SQUID magnetometer with a 500 Oe external magnetic field. The diamagnetic corrections of the molar magnetic susceptibilities were applied using Pascal's constants. The EPR spectrum was recorded for the polycrystalline sample at room temperature on a Bruker BioSpin GmbH spectrometer.

2.2. Syntheses

The ligands N^2-(pyrazin-2-yl)-N^6-(6-(pyrazin-2-ylamino) pyridin-2-yl)pyridine-2,6-diamine (H_3pzpz) and N^2-(pyrazin-2-yl)-N^6-(6-(pyridin-2-ylamino)pyridin-2-yl)pyridine-2,6-diamine (H_3tpz) were synthesized using Buchwald's palladium-catalyzed methods as documented in the literature [27].

$[Cu(H_3pzpz)(NO_3)]\cdot NO_3\cdot H_2O$ (1). $Cu(NO_3)_2\cdot 3H_2O$ (0.532 g, 0.0022 mol) and H_3pzpz (0.714 g, 0.002 mol) were combined with methanol (50 mL) and agitated for 24 hours at room temperature. After filtering out insoluble contaminants, the mixture was vacuum-concentrated. After two weeks of slow evaporation of the concentrate, single green block crystals of **1**, appropriate for X-ray diffraction investigation, were obtained by filtering (1.060 g, 86% yield); IR (KBr) ν/cm^{-1}: 3250 w, 3200 w, 3050 w, 1642 m, 1576 m, 1543 s, 1427 vs, 1385 sh, m, 1308 s, 1215 m, 1148 s, 1032 m, 842 sh, m, 790 s, 659 w, 436 m; UV/Vis (CH_3OH) λ_{max}/nm (ε/dm^3 mol^{-1} cm^{-1}): 209 (2.13×10^4), 254 (1.28×10^4), 342 (1.23×10^4), 665 (1.12×10^2), 908 (1.03×10^2); Elemental analysis (%) $C_{18}H_{17}CuN_{11}O_7$: calc. C 38.40, H 3.04, N 27.37; found: C 38.32, H 3.12, N 27.43.

$[Cu(H_3tpz)Cl]_2\cdot 2(Cl)\cdot 5H_2O$ (2). A mixture of H_3tpz (0.358 g, 0.001 mol) and $CuCl_2\cdot 2H_2O$ (0.187 g, 0.0011 mol) in methanol (25 mL) was stirred at room temperature for 24 hours. Then the solution was filtered to remove insoluble impurities and concentrated under vacuum. The yellow-green solid compound was collected by filtration, after 6 hours. After being cleaned with a small amount of cold methanol, the final product was allowed to air dry. During nine days, block colourless crystals of **2** were obtained upon recrystallization from a methanol/water (2:1 v/v) solution at room temperature (0.475 g, 87% yield); IR (KBr) ν/cm^{-1}: 3391 br., 3295 w, 3198 w, 1640 m, 1580 s, 1543 m, 1431 vs, 1274 w, 1215 m, 1151 m, 1017 m, 775 br., s, 518 w, 424 m; UV/Vis (CH_3OH) λ_{max}/nm (ε/dm^3 mol^{-1} cm^{-1}): 210 (2.21×10^4), 252 (1.24×10^4), 326 (1.26×10^4), 674 (1.08×10^2), 903 (1.01×10^2); Elemental analysis (%) $C_{38}H_{42}Cl_4Cu_2N_{16}O_5$: calc. C 42.59, H 3.95, N 20.91; found: C 42.65, H 3.89, N 21.03.

2.3. The determination of antimicrobial activity

Complexes **1** and **2** were dissolved in DMSO to create 10 mg/mL stock solutions, which were then preserved at 4 °C. To prepare the nutrient agar (pH 7.2–7.4), 28 g of the commercial powder was mixed into 1000 mL of distilled water and sterilized via autoclaving at 121 °C for 15 minutes. The antimicrobial efficacy of the samples was tested against *P. aeruginosa* (ATCC 27853), *M. phlei* (ATCC 11758), *A. niger* (ATCC 16404), and *P. chrysogenum* (ATCC 10106) using the agar well diffusion technique. Nutrient agar plates were inoculated with bacterial (10^8 CFU/mL) or fungal (10^6 spores/mL) suspensions, followed by the introduction of 100 μL of test compounds (100 μg/mL) into 6 mm diameter wells. Inoculated plates were maintained at 37 °C for 24 hours for bacterial cultivation, while fungal cultures were incubated at 28 °C for 48–72 hours. The resulting inhibition zones were measured in triplicate using a digital caliper. Ciprofloxacin (5 μg/disc) and nystatin (100 units/disc) acted as positive controls; dimethyl sulfoxide (DMSO) and sterile distilled water were used as negative and blank controls, respectively.

2.4. Crystal structure determinations

The appropriate crystals of **1** and **2** were chosen for data collection, which was carried out using Mo-Kα radiation (λ=0.71073 Å) on a D8-QUEST diffractometer at 293 K. SHELXS-2013 [28] was used to solve the structure directly, and SHELXL-2013 [29] was used to improve it using full-matrix least-squares techniques on F2. Anisotropic parameters

were used to refine all non-hydrogen atoms. Following their location on several maps, the hydrogen atoms were identified as riding atoms with a C-H distance of 0.93 Å and an N-H distance of 0.86 Å. The locations of the other H atoms were found in a freely refined difference map. MERCURY software were used to produce molecular visualizations. Table 1 provides the primary crystallographic information of the complexes as well as the specifics of the X-ray diffraction experiment.

3. Results and discussion

3.1. Syntheses and structures

The complexes $[Cu(H_3pzpz)(NO_3)]\cdot NO_3\cdot H_2O$ (**1**) and $[Cu(H_3tpz)Cl]_2\cdot 2(Cl)\cdot 5H_2O$ (**2**) were synthesized by direct reactions of H_3pzpz and H_3tpz with $Cu(NO_3)_2\cdot 3H_2O$ and $CuCl_2\cdot 2H_2O$ in methanol, respectively. Single-crystal X-ray diffraction analysis revealed that the crystal structure of complex **1** is classified within the monoclinic system, specifically belonging to the space group $P2_1/c$. The molecular structure of the complex, including the atom numbering scheme, is depicted in figure 1.

The copper complexes $[Cu(H_3pzpz)(NO_3)]\cdot NO_3\cdot H_2O$ (**1**) and $[Cu(H_3tpz)Cl]_2\cdot 2Cl\cdot 5H_2O$ (**2**) were generated through the treatment of H_3pzpz and H_3tpz with $Cu(NO_3)_2\cdot 3H_2O$ and $CuCl_2\cdot 2H_2O$, respectively, in methanol. X-ray crystallographic studies confirmed that complex **1** adopts a monoclinic system, space group $P2_1/c$. Figure 1 presents the molecular structure of the complex, complete with the atom-numbering convention.

Table 1

Crystal data for 1 and 2

	1	**2**
Formula	$C_{18}H_{17}CuN_{11}O_7$	$2(C_{19}H_{16}ClCuN_8)\cdot 2(Cl)\cdot 5(H_2O)$
Formula weight Temperature (K)	562.96 293	1071.75 293
Crystal system	Monoclinic	Monoclinic
Space group	$P2_1/c$	$C2/c$
a (Å)	15.1860 (9)	13.3234 (10)
b (Å)	19.9896 (12)	25.713 (2)
c (Å)	7.5403 (4)	13.971 (1)
β (°)	101.034 (2)	101.823 (2)
V (Å^3)/Z	2246.6 (2)/4	4684.7 (7)/4
D_c (Mgm^{-3})	1.664	1.520
Absorption coefficient (mm^{-1})	1.04	1.20
Crystal size (mm)	0.13×0.09×0.04	0.05×0.04×0.02
θ range for data collection (°)	2.7–22.3	2.2–23.0
Reflection collected	38017	40799
Independent reflections	4623 (R_{int}=0.070)	4899 (R_{int}=0.055)
R_F, $R_W(F^2)$ (I>2σ(I))	0.065, 0.139	0.055, 0.147
R_F, $R_W(F^2)$ (all data)	0.119, 0.166	0.090, 0.170
GOF	1.02	1.09

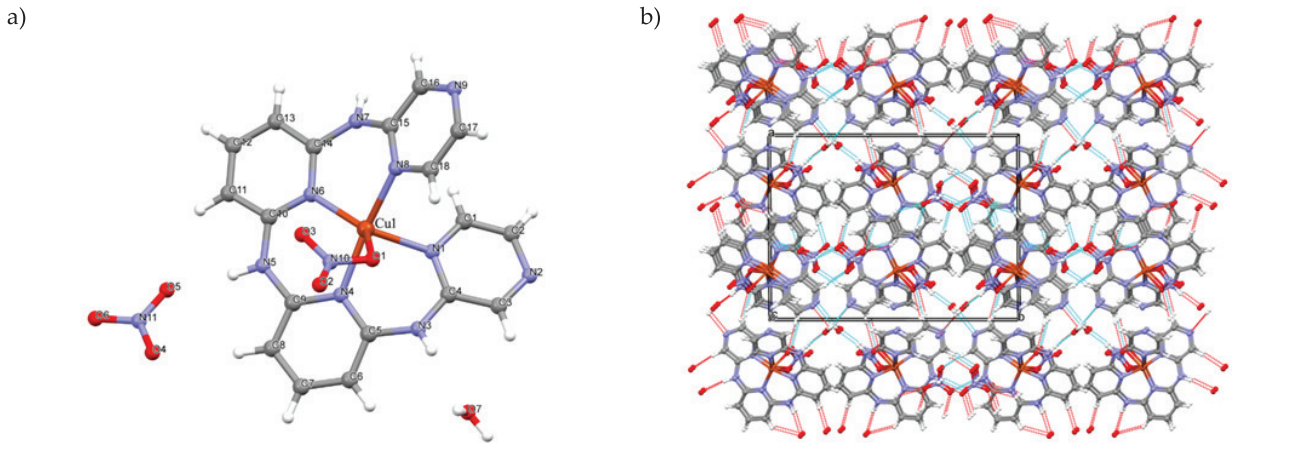

Fig. 1. The molecular structure of the complex 1: a) The crystal structure of $[Cu(H_3pzpz)(NO_3)]\cdot NO_3\cdot H_2O$ (1) is depicted, with probability thermal ellipsoids shown at the 40% level; b) The 3D infinite supramolecular network in (1) is illustrated, which is formed by hydrogen bonds

Details of the X-ray structural analysis experiment and the main crystallographic data for compound **1** are provided in table 1. Selected interatomic distances and valence angles of the complex are listed in table 2. In the crystal lattice of compound **1**, contains one water molecule present. The complex described as **1** is a mononuclear and neutral entity, where the central Cu(II) atom is coordinated to five heteroatoms in an N_4O environment. The geometry around Cu1 is best described as distorted trigonal bipyramidal. The trigonality index τ is calculated by analyzing the largest α and β angles around the Cu(II) ion (where τ=0 and 1 for the perfect square pyramidal and trigonal bipyramidal geometries, respectively), and it was found to be 0.64 for complex **1** [30]. This arrangement is formed by the nitrogen atoms from two pyridine and two pyrazine rings of the H_3pzpz ligand, along with one oxygen atom from a mono-coordinated nitrate ion (fig. 1a). In this case, pyridine nitrogen atoms (N4, N6) and nitrate oxygen atoms (O1) are engaged in the equatorial plane, while the terminal pyrazine ring's nitrogen atoms (N1, N8) occupy the apical position. The short Cu–N distances (Cu(1)–N(1)=2.052(4) Å; Cu(1)–N(4)=1.968(4) Å; Cu(1)–N(6)=2.010(4) Å; Cu(1)–N(8)=1.977(4) Å) all show a strong chelating ligand binding and are in good agreement with the corresponding distances of copper complexes with modulated oligo-α-aminopyridine ligands [31-33]. Cu(1)–O(1) (2.331(4) Å) is comparatively lengthy, indicating weak bonding. As a quadridentate ligand, compound **1**'s H_3pzpz coordinates with the Cu(II) ion in an all-anti configuration. Coordination does not include the amido groups. The pyridine and pyrazine groups of the ligand are planar. The dihedral angles between (Pz(N1)-Py(N4)), (Py(N4)-Py(N6)), and (Py(N6)-Pz(N8)) are 25.28(3)°, 10.32(2)°, and 24.06(2)° for complex **1**. Complex **1** showed a large number of hydrogen bonds. Within the crystal lattice, amino groups, an uncoordinated nitrate anion, and a water molecule are all connected via intermolecular hydrogen bonds (HBs). These interactions' distances are as follows: N(5)···O(5)=2.850(6) Å, N(7)···O(4)=2.904 Å, and N(3)···O(7)=2.906(7) Å. These interactions help complex **1** create a three-dimensional network (fig. 1b). The analysis of the crystal structure of compound **1** using PLATON indicates the presence of intermolecular π-π stacking interactions. The distance between the centroid of Ring (I) and the centroid of Ring (J) is measured at 3.9352 (2) Å. Moreover, the distance between Cg(I) and the perpendicular projection of Cg(J) on Ring I is 3.207 Å. Hydrogen bonds and π-π stacking interactions contribute to overall system stability [34, 35].

Single-crystal X-ray diffraction analysis revealed that the crystal of complex **2** is classified within the monoclinic system, specifically in the space group C2/c. The molecular structure of complex **2** is illustrated in figure 2.

The Cu(1) atom in complex **2** is coordinated by four nitrogen atoms (N(1), N(4), N(6), and N(8)) derived from the H_3tpz ligand, as well as a chlorine atom (Cl1) from the coordinated chloride anion, resulting in a distorted trigonal bipyramidal geometry. The corners of the triangular base are occupied by two nitrogen atoms and one chlorine atom, while the axial positions of the trigonal bipyramidal structure are occupied by the two remaining nitrogen atoms. The crystal structure of compound **2** includes one noncoordinated chloride anion that acts as a counter-ion. Additionally, the crystal lattice contains five uncoordinated water molecules. Between 1.985(3) and 2.031(4) Å, the Cu–N distances are well within the range reported for Cu(II) complexes of oligo-α-aminopyridine ligands modified with nitrogen-containing heterocycles, including naphthyridine, pyrazine, and pyrimidine [31, 33]. Cu–Cl(1)'s comparatively large distance (2.5622(12) Å) suggests a weak connection. The H_3tpz ligand, similar to H_3teptra complexes, coordinates with Cu(II) in an all-anti configuration, acting as a quadridentate ligand [36]. The four pyridyl/pyrazyl groups of the H_3tpz ligand are planar, with adjacent pyridyl/pyrazyl planes

Table 2

Selected bond distances (Å) and angles (°) for 1 and 2

1			
Cu(1)–N(1)	2.052 (4)	Cu(1)–N(8)	1.977 (4)
Cu(1)–N(4)	1.968 (4)	Cu(1)–O(1)	2.331 (4)
Cu(1)–N(6)	2.010 (4)		
N(4)–Cu(1)–N(1)	88.88 (17)	N(8)–Cu(1)–N(6)	92.81 (16)
N(4)–Cu(1)–N(6)	96.05 (16)	N(1)–Cu(1)–O(1)	97.85 (17)
N(4)–Cu(1)–N(8)	169.84 (17)	N(4)–Cu(1)–O(1)	81.20 (17)
N(6)–Cu(1)–N(1)	131.24 (17)	N(6)–Cu(1)–O(1)	130.88 (17)
N(8)–Cu(1)–N(1)	89.01 (17)	N(8)–Cu(1)–O(1)	89.25 (17)
2			
Cu(1)–N(1)	2.001 (4)	Cu(1)–N(8)	2.031 (4)
Cu(1)–N(4)	2.030 (4)	Cu(1)–Cl(1)	2.5622 (12)
Cu(1)–N(6)	1.985 (3)		
N(1)–Cu(1)–N(4)	91.80 (14)	N(6)–Cu(1)–N(1)	170.25 (15)
N(1)–Cu(1)–N(8)	89.79 (14)	N(6)–Cu(1)–N(4)	95.28 (14)
N(1)–Cu(1)–Cl(1)	88.38(11)	N(6)–Cu(1)–N(8)	89.86 (14)
N(4)–Cu(1)–N(8)	135.45 (15)	N(6)–Cu(1)–Cl(1)	82.73 (11)
N(4)–Cu(1)–Cl(1)	113.24 (11)	N(8)–Cu(1)–Cl(1)	111.31 (11)

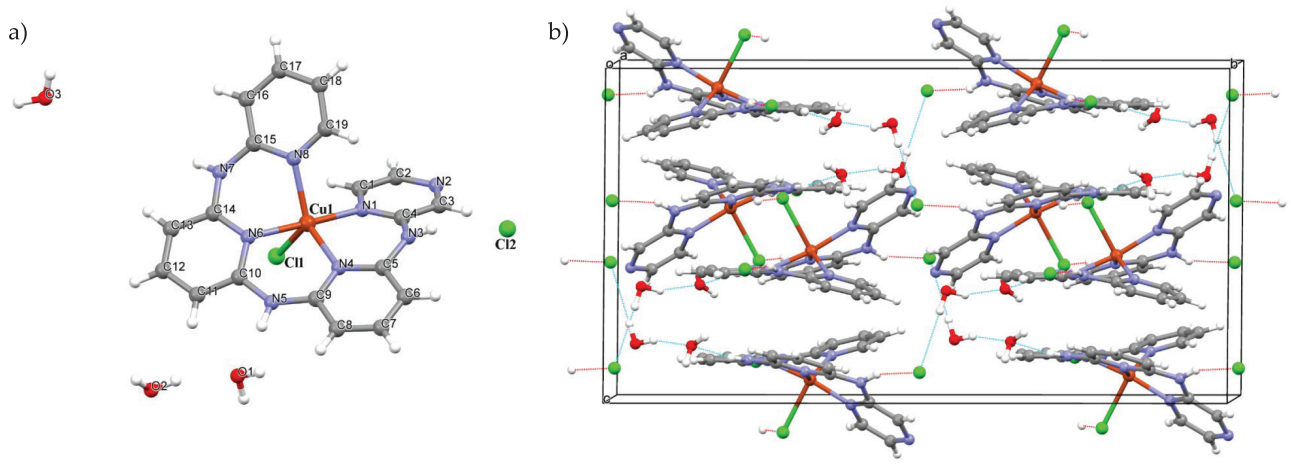

Fig. 2. The molecular structure of complex 2: a) Crystal structure and atom numbering scheme of $[Cu(H_3tpz)(Cl)]_2 \cdot 2(Cl) \cdot 5H_2O$ (2). The 30% probability threshold is used to illustrate thermal ellipsoids; b) The representation of a three-dimensional supramolecular structure in (2).

exhibiting dihedral angles of 23.76(2)° (Pz(N1)-Py(N4)), 16.70(2)° (Py(N4)-Py(N6)), and 17.49(2)° (Py(N6)-Pz(N8)). As listed in table 3, the structure features numerous classical N–H···Cl, N–H···O, and O–H···O hydrogen bonds. In this arrangement, the uncoordinated NH group of the H_3tpz ligand participates in intermolecular hydrogen bonding with the oxygen atoms of uncoordinated water molecules and uncoordinated chloride anions, among others. In addition, π–π stacking interactions between two neighboring π-systems formed by the aromatic rings of H_3tpz may play a role in enhancing the crystal stability of the complex. Complex **2** exhibits two intermolecular π-π stacking interactions, and the distances between stacked aromatic planes are 3.9350(3) and 3.6441(3) Å.

3.2. IR, UV-Vis, EPR spectroscopy and magnetic properties

The strong absorption bands observed in the IR spectra of complexes **1** and **2**, specifically in the range of 1427–1642 cm^{-1} (see fig. 3), are attributed to the C=C and C=N vibrations

Table 3

Hydrogen-bond geometry (Å, °) for complex 2

D–H···A	D–H	H···A	D···A	D–H···A
N3–H3A···Cl2	0.86	2.39	3.194 (4)	157
N5–H5···O1	0.86	2.00	2.859(5)	172
N7–H7A···Cl1^{i}	0.86	2.42	3.254(4)	164
O1–H1B···N3^{ii}	0.85	2.56	2.385(6)	165
O2–H2B···Cl2^{i}	0.88	2.74	3.617(10)	178
Symmetry codes: (i) –x+1/2, –y+1/2, -z+1; (ii) -x+3/2, –y+1/2, -z+1				

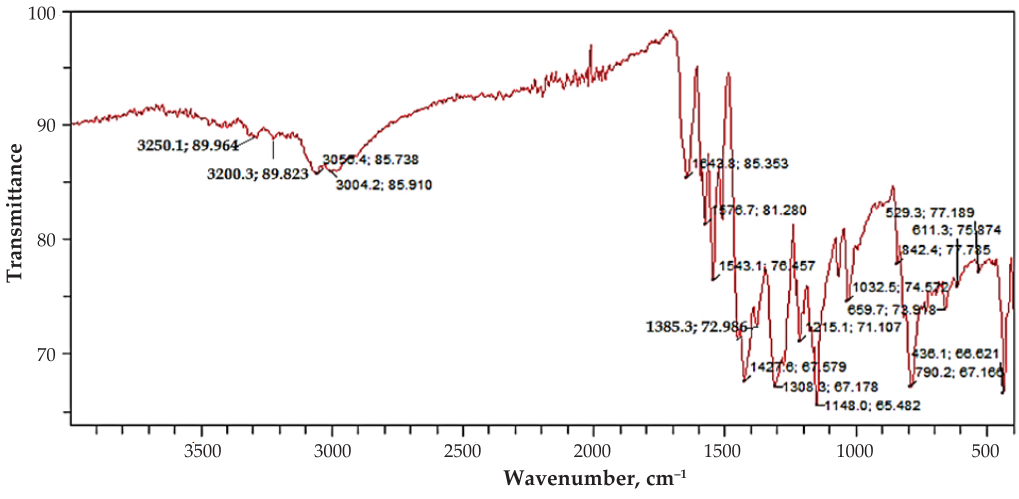

Fig. 3. IR spectra of complex 1

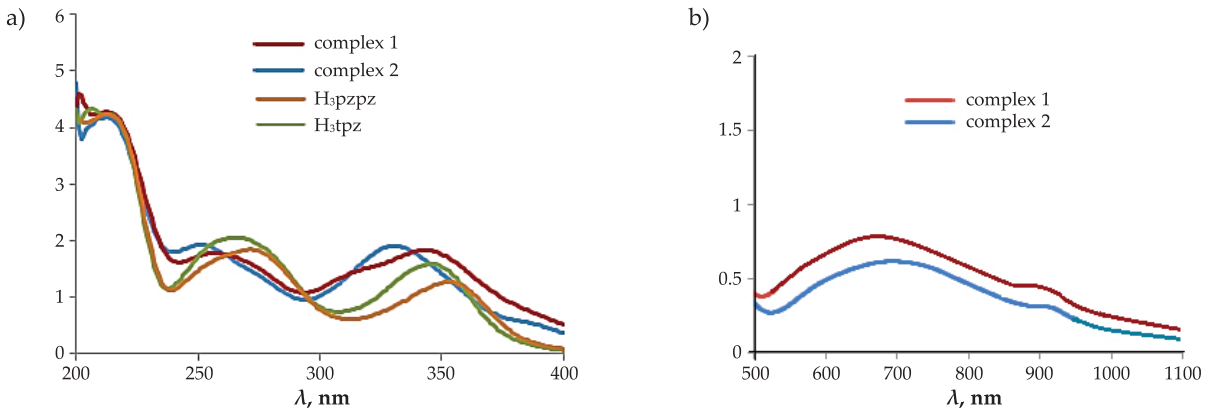

Fig. 4. The electronic spectra of the H_3pzpz and H_3tpz ligands, and their corresponding complexes 1 and 2, measured in a methanol solution

associated with the pyridyl and pyrazyl groups. The NH bonds of amine groups are represented by the band groups at 3198–3295 cm^{-1}, which clearly demonstrate that the nitrogen atoms of amino groups are not coordinated with metal centers in either combination. As a result, the infrared spectra of the H_3pzpz ligand at 3117–3278 cm^{-1} and the H_3tpz ligand at 3106–3262 cm^{-1}, as well as those of its complexes **1** and **2**, do not show any discernible differences. Tentatively, the two new bands seen at 436 and 424 cm^{-1} are attributed to ν_a(Cu–N) of complexes 1 and 2, respectively. In complex **1**, the coordinated nitrate anion displayed distinctive strong vibrations at 1427 cm^{-1} for $\nu_a(NO_2)$, 1308 cm^{-1} for $\nu_s(NO_2)$, and 1032 cm^{-1} for ν(NO). At the same time, the existence of the uncoordinated nitrate ions in the complex is indicated by the presence of a medium-intensity band at 842 cm^{-1} and a strong band at 1385 cm^{-1} (which appears as a shoulder) in the infrared spectrum. The results obtained align well with the X-ray crystal structure studies of these compounds. Previous reports have documented other Cu(II) nitrate complexes with nitrogen-containing ligands exhibiting a similar binding mode for the NO_3^- anion [22, 37, 38].

In the electronic spectra of complexes **1** and **2** in the UV region with the H_3pzpz and H_3tpz ligands, a number of absorption bands associated with the $\pi \rightarrow \pi^1$ and $n \rightarrow \pi$ transitions of the ligands are observed (fig. 4). Two spin-allowed transitions are anticipated in the visible or near-infrared spectrum of trigonal-bipyramidal copper(II) complexes [39]. Indeed, the electronic spectrum of compound **1** in methanol solution shows two *d-d* transitions at 665 and 908 nm. It would be correct to attribute the lower energy band at 908 nm to the d_{xy}, $d_{x^2-y^2} \rightarrow d_{z^2}$ transitions and the higher energy band at 665 nm to the d_{xz}, $d_{yz} \rightarrow d_{z^2}$ transitions, following the studies [40, 41] discussed in the literature. The results obtained are consistent with a trigonal-bipyramidal ligand environment for the Cu(II) ions in **1**, which is further supported by X-ray structural analysis. Similar results are obtained in studying the electronic spectra of complex **2**, which has two *d-d* transitions at 674 and 903 nm. These results also confirm the trigonal bipyramidal structure of this complex.

To obtain more evidence regarding the geometry of Cu(II) ions in complexes **1** and **2**, EPR study was performed. Two distinct geometric configurations are possible in synthesized pentacoordinated Cu(II) complexes—**1** and **2** for Cu(II)N_4X (X=O for **1**; Cl for **2**) polyhedrons: the square pyramidal geometry (SP) (symmetry D_{4v}) and the trigonal bipyramidal geometry (TBP) (symmetry D_{3h}). The powder solid-state EPR spectra of complexes **1** and **2** were recorded at room temperature. The EPR spectrum of 1, which is typical for a powder sample, is displayed in figure 5. The EPR spectrum of **1** is the «inverted type» with $g_{paral} < g_{perp}$. It exhibits the typical Cu^{2+} ion anisotropic pattern (S=1/2, I=3/2). Both parallel and perpendicular components are identified in this spectrum. Spin-orbital and spin-exchange interactions produced line broadening due to the increasing spin concentration, making it difficult to resolve hyperfine splitting. The values of the $g_\parallel$ and $g_\perp$ components were calculated from the powder spectrum. These parameters have the following numerical values: $g_\perp$=2.159 and $g_\parallel$=2.016. The g parameters indicate axial symmetry in the paramagnetic core. Complex **2** shows extremely near values of $g_\parallel$ and $g_\perp$ components of the g tensor ($g_\parallel$=2.003 and $g_\perp$=2.183) and a comparable EPR spectrum. Cu(II) ions are found in the distorted triangular bipyramid structure, and the ground state of the unpaired electron is d_z^2, according to the order of $g_\perp > g_\parallel \sim g_e$ (free electron g value, g_e=2.0023) [29]. For complexes **1** and **2**, the EPR results show excellent agreement with the data from single crystal analysis (table 2). For the complexes of **1** and **2**, the observed magnetic moments at 300 K are 1.79 and 1.82 B.M., which are compatible with one unpaired electron in Cu(II) (d^9), including a small orbital contribution.

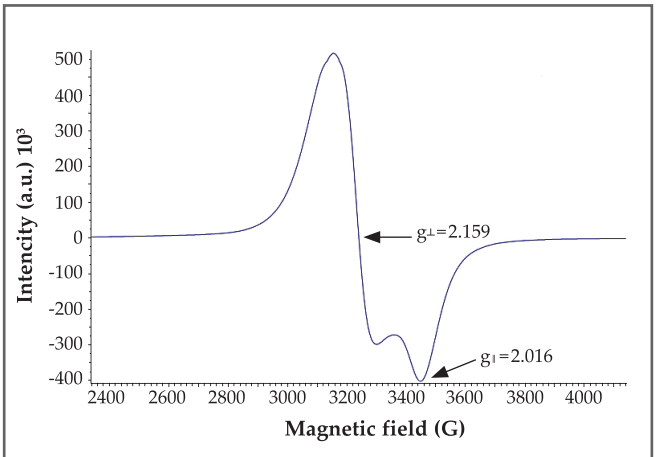

Fig. 5. EPR spectra of powder sample of the copper(II) complex 1 at room temperature

[1]Values represent mean ± standard deviation of three independent experiments. The zone diameter includes 6 mm well.

3.3. Antibacterial and antifungal activities on nutrient agar

3.3.1. Antibacterial activity on nutrient agar

The antibacterial activity results obtained on nutrient agar medium are presented in table 4.

Both mononuclear copper(II) complexes demonstrated significant antibacterial activity on nutrient agar. complex **2** exhibited superior activity against *P. aeruginosa* (26 mm) compared to complex **1** (20 mm). *Against M. phlei*, complex **2** produced an inhibition zone of 22 mm, while complex **1** showed 16 mm. The free ligands displayed minimal activity (8–12 mm), indicating that copper coordination is essential for antimicrobial efficacy.

3.3.2. Antifungal activity on nutrient agar

The antifungal activity results are summarized in table 5.

Both mononuclear complexes exhibited significant antifungal activity on nutrient agar. Complex **2** showed greater potency against *A. niger* (21 mm) and *P. chrysogenum* (18 mm) compared to complex **1** (17 mm and 14 mm, respectively). The free ligands demonstrated minimal antifungal activity (7–9 mm).

3.4. Comparative activity profile

The antimicrobial activity profile on nutrient agar revealed that both mononuclear complexes were most effective against *P. aeruginosa*, followed by *M. phlei*, *A. niger*, and *P. chrysogenum.* Complex **2** consistently outperformed complex **1** across all tested strains, with activity enhancements of 23–30 % relative to complex **1**, despite both being mononuclear species.

The high redox activity and ROS generation capability of complex **2** open possibilities for catalytic applications in the selective oxidation of hydrocarbons during petroleum refining, particularly in oxidative desulfurization (ODS) processes where thiophene-type sulfur compounds are oxidized and removed. The stability of copper complexes under the high-salinity and high-temperature conditions of petroleum environments makes them promising candidates for use as antimicrobial agents and corrosion inhibitors in reservoir fluids, as the $Htpz^{2-}$ and $Hpzpz^{2-}$ ligands can engage in π-π interactions with the aromatic components of crude oil [42, 43].

Table 4

Antibacterial activity of mononuclear copper(II) complexes on nutrient agar (zone of inhibition, mm)

Compound	Concentration (μg/mL)	*P. aeruginosa* ATCC 27853	*M. phlei* ATCC 11758
H_3tpz	100	10 ± 0.5	8 ± 0.4
H_3pzpz	100	12 ± 0.6	9 ± 0.5
Complex 1	100	20 ± 1.0	16 ± 0.8
Complex 2	100	26 ± 1.2	22 ± 1.0
Ciprofloxacin	5 μg/disc	30 ± 1.0	28 ± 1.2
DMSO	-	0	0

Table 5

Antifungal activity of mononuclear copper(II) complexes on nutrient agar (zone of inhibition, mm)

Compound	Concentration (μg/mL)	*A. niger* ATCC 16404	*P. chrysogenum* ATCC 10106
H_3tpz	100	8 ± 0.3	7 ± 0.2
H_3pzpz	100	9 ± 0.4	8 ± 0.3
Complex 1	100	17 ± 0.8	14 ± 0.7
Complex 2	100	21 ± 1.0	18 ± 0.9
Nystatin	100 units/disc	24 ± 1.0	22 ± 0.9
DMSO	-	0	0

Conclusions

Using pyrazine-modulated oligo-α-pyridylamine ligands, specifically N^2-(pyrazin-2-yl)-N^6-(6-(pyrazin-2-ylaminopyridin-2-yl)pyridin-2,6-diamine (H_3pzpz) and N^2-(pyrazin-2-yl)-N6-(6-(pyridin-2-ylaminopyridin-2-yl)pyridin-2,6-diamine (H_3tpz), two new mononuclear copper(II) complexes were synthesized and structurally characterized: $[Cu(H_3pzpz)(NO_3)]\cdot NO_3\cdot H_2O$ (**1**) and $[Cu(H_3tpz)Cl]_2\cdot 2(Cl)\cdot 5H_2O$ (**2**). In both complexes, H_3pzpz or H_3tpz acts as a tetradentate ligand; it coordinates the copper(II) ion in an all-anti conformation, and the Cu(II) atom is five-coordinated in a distorted trigonal bipyramidal geometry. The distorted trigonal bipyramidal structure of the synthesized compounds is well compatible with two spin-allowed transitions in the visible portion of their electronic spectra, as well as with the «inverted type» EPR spectra where g_{paral} is less than g_{perp}. In complexes **1** and **2**, extensive hydrogen bonds and intermolecular π-π interactions create a three-dimensional network that stabilizes the crystal packing. Synthesized complexes exhibited significant antimicrobial activity against four pathogenic strains, with **2** superior to **1** (zones 18–26 mm vs. 14–20 mm). This demonstrates that antimicrobial efficacy in mononuclear systems is governed by coordination sphere engineering—coligand identity, crystal packing, and geometry—rather than nuclearity, guiding rational metallodrug design. Furthermore, the demonstrated redox versatility and sulfur-binding capability of these copper(II) complexes suggest promising applications in petroleum chemistry, particularly as potential catalysts for oxidative desulfurization processes and as dual-function antimicrobial-corrosion inhibitors in oilfield environments where microbial proliferation accelerates pipeline degradation.

Supplementary data

The further crystallographic information for complexes 1 and 2 is available from CCDC 2422938 and 2536545. The Cambridge Crystallographic Data Centre at 12 Union Road, Cambridge CB2 1EZ, UK, or the website http://www.ccdc.cam.ac.uk/conts/retrieving.html *are two ways to acquire this data free of charge. They can also be contacted via email at deposit@ccdc.cam.ac.uk or by fax at (+44) 1223-336-033.*

References

1. Cotton, F. A., Murillo, C. A., Walton, R. A. (2005). Multiple bonds between metal atoms. 3rd Ed. Ch.15. *New York: Springer*.

2. Peng, S. M., Wang, C. C., Jang, Y. L., et al. (2000). One- dimensional metal string complexes. *Journal of Magnetism and Magnetic Material*, 209, 80–83.

3. Ismayilov, R. H., Ismayilova, S. Z., Tagiyev, D. B., et al. (2025). Linear nonanuclear chromium(II) complex with pyrazine-modulated pentapyridyltetraamine ligand: Synthesis, structure and properties. *Journal of Molecular Structure*, 1331, 141592.

4. Brogden, D. W., Berry, J. F. (2015). Coordination chemistry of 2, 2′-dipyridylamine: The gift that keeps on giving. *Comments on Inorganic Chemistry*, 36(1), 17-37.

5. Wu, F., Tong, H., Wang, K., et al. (2016). Synthesis, structural characterization and photophysical studies of luminescent Cu(I) heteroleptic complexes based on dipyridylamine. *Journal of Photochemistry and Photobiology A: Chemistr*, 318, 97–103.

6. Chung, Y. H., Lin, H. H., Wei, H. H. (2005). Synthesis, crystal structure, and magnetic properties of (2,2′-dipyridylamine)(X^-) copper(II) complexes (X: cyanate, dicyanamide, acetate, thiocyanato). *Journal of the Chinese Chemical Society*, 52, 877-884.

7. Schodel, H., Nather, C., Bock, H., Butenschon, F. (1996). Trimorphism of 2,2'-dipyridylamine: Structures, phase transitions and thermodynamic stabilities. *Acta Crystallographica Section B*, 52, 842-853.

8. Ismayilov, R. H., Valiyev, F. F., Israfilov, N. V., et al. (2020). Long chain defective metal string complex with modulated oligo-á-pyridylamino ligand: Synthesis, crystal structure and properties. *Journal of Molecular Structure*, 1200, 126998.

9. Wang, W. Z., Ismayilov, R. H., Lee, G. H., et al. (2012). Fine tuning of pentachromium(II) metal string complexes through elaborate design of ligand. *New Journal of Chemistry*, 36, 632–637.

10. Ismayilova, S. Z., Guliyeva, L. Sh., Ismayilov, R. H., et al. (2025). Synthesis and structure of the novel mononuclear copper(II) complex of the unsymmetrical pyrimidine-modulated long-chain hexapyridylpentaamine ligand. *Eurasian Journal of Chemistry*, 30(4(120)), 79–87.

11. Ismayilova, S. Z., Ismayilov, R. H., Tagiyev, D. B., et al. (2025). Copper(II) complex of the pyrazine-modulated oligo-α-aminopyridine as a coordination polymers' promising building block. *Chemical Problems*, 4(23), 476-482.

12. Guliyeva, E. A. A., Mejidov, A. A., Ismayilov, R. H., et al. (2026). Synthesis, structure, and properties of a polymeric copper(II) complex with anion of maleic acid. *Transition Metal Chemistry*, 51, 16.

13. Suleimanov, B. A., Abbasov, H. F., Ismayilov, R. H. (2023). Thermophysical properties of suspensions with $[NI_3(\mu_3\text{-PPZA})_4CL_2]$ metal string complex microparticles. *SOCAR Proceedings*, 1, 194-204.

14. Tantawy, E. S., Amer, A. M., Mohamed, E. K., et al. (2020). Synthesis, characterization of some pyrazine derivatives as anti-cancer agents: In vitro and in silico approaches. *Journal of Molecular Structure*, 1210, 128013.

15. Choudhary, D., Garg, S., Kaur, M., et al. (2023). Advances in the synthesis and bio-applications of pyrazine derivatives: A review. *Polycyclic Aromatic Compounds*, 43, 4512–4578.

16. Ong, K. T., Liu, Z. Q., Meng, G. T. (2017). Review on the synthesis of pyrazine and its derivatives. *Borneo Journal of Resource Science and Technology*, 7, 60–75.

17. Huigens, R. W., Brummel, B. R., Tenneti, S., et al. (2022). Pyrazine and phenazine heterocycles: Platforms for total synthesis and drug discovery. *Molecules*, 27(3), 1112.

18. Qi, J., Wang, X., Liu, T., et al. (2020). Synthesis, antiproliferative activity and mechanism of copper(II)-thiosemicarbazone complexes as potential anticancer and antimicrobial agents. *Journal of Coordination Chemistry*, 73(7), 1208-1221.

19. Vinayagam, V., Prabu, S., Rajalakshmi, S., Arumugam, M. N. (2023). Synthesis, characterization, DNA interaction, antimicrobial activity, DFT analysis and molecular docking studies of copper(II) complex with triazine and neocuproine. *Journal of Molecular Structure*, 1287, 135649.

20. Ismayilova, S. Z., Ismayilov, R. H., Tagiyev, D. B., et al. (2025). Copper(II) monohelix complexes with pyrazine-modulated long-chain oligo-α-aminopyridine ligand: synthesis, crystal structures, and bioactivity studies. *Journal of Molecular Structure*, 1347, 143295.

21. Ismayilov, R. H., Valiyev, F. F., Tagiyev, D. B., et al. (2024). Trinuclear nickel (II) string complexes and copper (II) coordination polymer with pyrazine modulated unsymmetrical dipyridylamino ligand: Synthesis, structure and bioactivity properties with molecular docking. *Journal of Molecular Structure*, 1307, 137966.

22. Abbasova, G. G., Ismayilov, R. H., Tagiyev, D. B., et al. (2024). Synthesis, characterization, crystal structure, molecular dynamics simulations, MM-GBSA analysis, and bioactivity studies of pyrazine- and pyrimidine-modulated unsymmetrical dipyridylamide complexes. *Journal of Molecular Structure*, 1315, 138896.

23. Lister, P. D., Wolter, D. J., Hanson, N. D. (2009). Antibacterial-resistant pseudomonas aeruginosa: clinical impact and complex regulation of chromosomally encoded resistance mechanisms. *Clinical Microbiology Reviews*, 22(4), 582-610.

24. Lemire, J. A., Harrison, J. J., Turner, R. J. (2013). Antimicrobial activity of metals: mechanisms, molecular targets and applications. *Nature Reviews Microbiology*, 11(6), 371-384.

25. MacFaddin, J. F. (1985). Media for isolation-cultivation-identification-maintenance of medical bacteria. Vol.1. *Baltimore: Williams & Wilkins.*

26. Li, X., Ai, S., Huang, Y., et al. (2021). Fast and reversible adsorption for dibenzothiophene in fuel oils with metallic nano-copper supported on mesoporous silica. *Environmental Science and Pollution Research*, 28(3), 2741–2752.

27. Wang, W. Z., Ismayilov, R. H., Lee, G. H., et al. (2007). The nano-scale molecule with the longest delocalized metal–metal bonds: linear heptacobalt(II) metal string complexes $[Co_7(\mu_7\text{-L})_4X_2]$. *Dalton Transactions*, 8, 830–839.

28. Sheldrick, G. M. (2008). A short history of SHELX. *Acta Crystallographica*, A64, 112.

29. Sheldrick, G. M. (2015). Crystal structure refinement with SHELXL. *Acta Crystallographica*, C71, 3.

30. Korkmaz, Ş. A., Karadağ, A., Yerli, Y., Soylu, M. S. (2014). Synthesis and characterization of new heterometallic cyanido complexes based on $[Co(CN)_6]^{3-}$ building blocks: crystal structure of $[Cu_2(N\text{-bishydeten})_2Co(CN)_6]\cdot 3H_2O$ having a strong antiferromagnetic exchange. *New Journal of Chemistry*, 38, 5402-5410.

31. Ismayilov, R. H., Wang, W. Z., Lee, G. H., et al. (2007). New versatile ligand family, pyrazine-modulated oligo-a-pyridylamino ligands, from coordination polymer to extended metal atom chains. *Dalton Transactions*, 27, 2898–2907.

32. Muley, A., Kumbhakar, S., Raut, R., et al. (2024). Mononuclear copper(II) complexes with polypyridyl ligands: synthesis, characterization, DNA interactions/cleavages and in vitro cytotoxicity towards human cancer cells. *Dalton Transactions*, 53(28), 11697-11712.

33. Lu, L. P., Zhu, M. L., Yang, P. (2004). Chloro(L-glutamato-k^2N,O)(1,10-phenanthroline-k^2N,N')copper(II) monohydrate. *Acta Crystallographica*, C60, m21-m23.

34. Spek, A. L. (2009). Structure validation in chemical crystallography. *Acta Crystallographica*, D65, 148–155.

35. Główka, M. L., Martynowski, D., Kozłowska, K. (1999). Stacking of six-membered aromatic rings in crystals. *Journal of Molecular Structure*, 474, 81-89.

36. Yang, M., Lin, T. W., Chou, C. C., et al. (1997). New oligo-a-pyridylamino ligands and their metal complexes. *Chemical Communications*, 23, 2279-2280.

37. Li, L., Dong, S., He, W., et al. (2023). Synthesis, crystal structures, electrochemistry and thermal stabilities of two copper complexes built by 3,7-di(3-pyridyl)-1,5-dioxa-3,7-diazacyclooctane. *Polyhedron*, 231, 116268.

38. Santoro, A., Mighell, A. D., Reimann, C. W. (1970). The crystal structure of a 1:1 cupric nitrate- pyrazine complex $Cu(NO_3)\cdot(C_4N_2H_4)$. *Acta Crystallographica Section B-Structural Science*, 26, 979.

39. Vicente, M., Bastida, R., Macías, A., et al. (2005). Copper complexes with new oxaaza-pendant-armed macrocyclic ligands: X-ray crystal structure of a macrocyclic copper(II) complex. *Inorganic Chimica Acta*, 358, 1141–1150.

40. Hathaway, B. J., Billing, D. E. (1970). The electronic properties and stereochemistry of mononuclear complexes of the copper(II) ion. *Coordination Chemistry Reviews*, 5, 143–207.

41. Chandra, S., Gupta, L. K. (2005). EPR, mass, IR, electronic, and magnetic studies on copper(II) complexes of semicarbazones and thiosemicarbazones. *Spectrochimica Acta Part A: Molecular and Biomolecular Spectroscopy*, 61(1-2), 269–275.

42. Mammadbayli, E. H., Ayyubov, I. H., Babayev, E. R. (2026). Study of optical activity of oils from the Zagly, Jafarly and Naftalan fields. *SOCAR Proceedings*, 1, 157-165.

43. Gasanov, A. H., Ayyubov, I. H., Aliyev, S. S., Babayev, E. R. (2024). Fuel hydrocarbons based on dicyclopentadiene: A short review. *SOCAR Proceedings*, 3, 98–106.